Chapter 3

Mechanical Properties and Deformation Behaviors of Metallic Glasses Investigated by Atomic-Level Simulations

Hongwei Zhao, Dan Zhao, Bo Zhu and Shunbo Wang

Additional information is available at the end of the chapter

http://dx.doi.org/10.5772/intechopen.76830

Abstract

The chapter reviewed recent developments about intrinsic structure of metallic glasses and their mechanical properties at atomic level, with an emphasis on making connections between developments in theory and simulations. Topics covered the following: structure analysis on metallic glasses with methods of pair distribution function, Honeycutt-Andersen analysis, and Voronoi tessellation; the connection of structure with the mechanical properties; shear band initiation and the development at the atomic level; and deformation mode transition from cast metallic glasses to reconstructed nanoglasses. These works provided theoretical understanding on the essence of metallic glasses' mechanical properties and deformation behaviors, and offered promises for more extensive applications of metallic glasses.

Keywords: metallic glasses, molecular dynamics simulation, shear bands, structure analysis, mechanical behavior

1. Introduction

Metallic glasses (MGs), also named amorphous alloys for their disordered atomic structure, behave excellent mechanical behaviors, including high elastic modulus, high yield stress, and extreme high hardness, compared with traditional crystalline alloys. Considering their excellent mechanical performance in micro-nano scale, MGs have a great application potential in ultra-precision systems. The research work on MGs has been proceeding for over 50 years

both experimentally and theoretically. Meanwhile, the corresponding simulation methods with aids of computer science have also been developed to provide assistance for the experimental research from the theoretical aspect. The most used simulation methods for the MGs are finite element method (FEM) and molecular dynamics (MD) method. FEM constructs a constitutive model of MG at the macroscopic scale on time and space, which is coincident with experimental works. For this advantage, it is usually employed to investigate the mechanical properties and shear bands (SBs) formation in the bulk MG systems [1–4]. Although a MG is usually regarded as isotropic and homogeneous from the macroscopic scale, a homogeneous constitutive model is not sufficient for the generation and localization of SBs in a typical brittle MG system. For the improvement, two different SB formation theories, free volume theory [1, 2] and shear transition zone (STZ) theory [3, 4] were employed in constitutive model to provide nucleation possibilities in the MG model, and they are proved quiet effective when depicting the formation process of SBs. However, these FEM simulations are basing on a fuzzy description of flow events according to the two immature theories, but neglect intrinsic dynamics of the flow events from atomic aspect. Furthermore, the theoretical frames and constitutive model for the research of MGs have to build on accurate description of their atomic structure. Since, the lack of effective experimental tools on characterizing the atomic structure of MGs, resolving the intrinsic structure only from experimental methods is unreasonable. Recently, MD methods are developed to offer possibility for the investigation on MGs from atomic level. By simulating the atoms movements and tracking atoms trajectories, MD simulation can calculate the basic thermal information of a MG ensemble, including temperature, potential energy, as well as some derived information such as atom shear stress, atom shear strain, and structure evolution and so on. Thus, MD simulation method is an effective tool when investigating the intrinsic structure of MG, and its connection with mechanical properties, as well as the elastic to plastic deformation transition.

In this chapter, we mainly take a review on the former research work on the connections between structure and properties in MGs. We began with the current understanding in the structure of MGs and then discuss their proper connection with some mechanical behaviors. Afterwards, more specific discussion on the SBs formation and development will be given based on various mechanics of MD simulations. Finally, based on the limitation of MGs in their applications, we discussed several multi-component materials derived from cast MGs, and have an outlook on the development trend of MG preparation and application.

2. Structure of metallic glasses

The essential feature of MG is considered as disordered, but there is still no exactly model to describe the total features of amorphous structure. The little research on the atomic structure of amorphous system, as well as the correlation of amorphous structure and mechanical behaviors, has obstructed the development on design and implication of amorphous materials seriously. Thus, the characterization and modeling of amorphous structure has been one of the most important and challenge research works in condense physics and material science area, and it is also the basis of research work on the mechanical behavior of MGs.

http://dx.doi.org/10.5772/intechopen.76830

The first model of atomic structure in MG was developed by Bernal, and it was described as a dense random packed structure of equal-sized spheres with the absence of medium-range and long-range order [5]. Bernal used the active hard balls to describe a liquid-like amorphous system, and analyzed the radial distribution function of the model, and found to have a good consistence with that of liquid system. This model provided a possibility of modeling and characterization based on the computer science. The further development of amorphous structure modeling has been based on Bernal's work, and more developed characterization methods have been raised from the aspects of statistic and topology with the aids of MD simulations. The most used characterization methods of MGs with MD simulation are presented as the following in this section, including pair distribution function, Honeycutt-Andersen analysis, and Voronoi tessellation method.

2.1. Pair distribution function

Pair distribution function (PDF) is the most classical and important statistical analysis method in amorphous systems; it is widely used in the characterization of liquids and amorphous materials. It is a pair correlation representing the probability of finding atoms, and described as a function of distance r from an average center atom. In a monatomic system, PDF is defined as:

$$g(r) = \frac{1}{4\pi r^2 \rho N} \sum_{i=1}^{N} \sum_{j=1, j\neq i}^{N} \delta\left(r - \left|\bar{r}_{ij}\right|\right), \tag{1}$$

where $\left|\bar{r}_{ij}\right|$ is the interatomic distance between atom i and atom j, and ρ is the number density of atoms in the system with N atoms. According to the PDF curve of a MG, the short-to-medium range order information can be manifested by the peak position, peak width, and relative intensity, etc. Conventionally, the nearest-neighbor shell atoms contribute to the first peak, which represents short range order (SRO) in the MG. A further distance up to 1–2 nm contributes the medium-range order (MRO). With distance r going larger, PDF gradually converges to unity, which means the atoms are randomly distributed, represents the long-range disorder. The structure evolution from liquid to glass can be shown from the PDF curves during the cooling procedure. **Figure 1** displays the PDF curves of a binary $Cu_{64}Zr_{36}$ MG in different temperature regions during its preparation process. It can be clearly seen that with decreasing temperature during quenching process, the second peak of total PDF gradually splits and becomes more pronounced, which indicates the formation of the glass phase and enhancement of SRO. Furthermore, the appearing temperature of the split is usually relevant to the glass transition temperature (T_g), indicating the generally formation and stability of the glass structure.

PDF is concise and clear for the characterization of amorphous materials, especially when detecting the amorphous phase transferred from a crystalline system; thus, PDF method is widely used to verify the effective MG models in MD simulations [6]. However, this method is only established on a statistic basis, without considering the exactly certain structure of MGs. It cannot provide the specific topology description of a certain amorphous system, thus has a limitation when further revealing the atomic structure geometry of MGs.

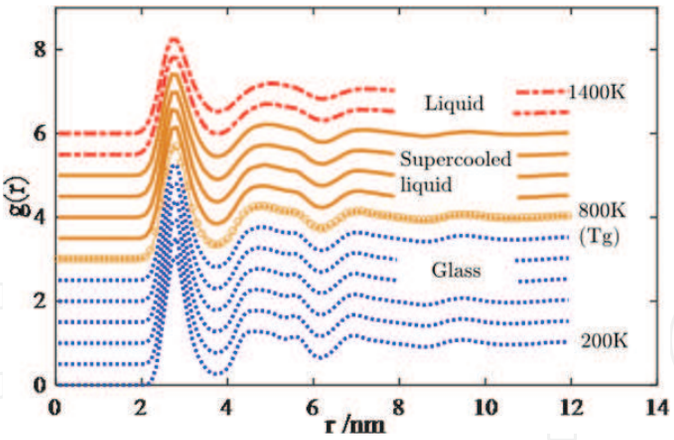

Figure 1. Partial distribution function of Cu-Zr MG during quenching process.

2.2. Honeycutt-Andersen analysis

A widely used and effective analysis method for the topology structure of crystalline systems is common neighbor analysis (CNA), which is proposed by Clarke and Jónsson [7]. CNA is mainly to describe a bonding correlation between neighboring atoms in highly regular ordered systems with integers *jkl*: (a) *j* for the number of near neighbors they have in common; (b) *k* for the number of bonds among the shared neighbors; (c) and *l* represents the number of bonds in the longest bonding chain in *k* type bonds. It can effectively detect general structure and abnormal structure in crystalline materials, but when used for various disordered structures, it cannot describe an accurate amorphous local structure and might have a misleading to structure analysis of MG.

Similar with CNA analysis method, Honeycutt-Andersen (H-A) analysis method uses a multiple integers *ijkl* to describe more unregularly ordered and complicated bond types [8]. The additional number *i* in the H-A indices *ijkl* indicates whether or not the near neighbors are bonded, $i = 1$ for bonded pairs and $i = 2$ for nonbonding atoms, and *l* is used to distinguish different bond geometries in case the first three numbers are same. The cutoff distance is derived from PDF curves for the particular pair of atoms. Different structures have different H-A indices to represent distinguished bond types. In the MGs, 1551 and 2331 are usually the characteristics of icosahedral ordering, which mainly contribute to SRO in MGs.

H-A indices can be employed to analyze SRO structures of MG. Duan et al. took the H-A analysis on $Cu_{50}Zr_{50}$ MG during the preparation process [9]. At the liquid state, the bond types with H-A indices 1441 and 1661 dominated the initial B2 phase crystalline model, and had the proportions 42 and 56%, respectively. When the temperature went to the totally melting liquid phase, the proportions dropped to 7 and 6%. The amorphous bond type 1431, 1541, and 1551 increased to 16, 12, and 14%, respectively. During a quenching process, the amorphous H-A indices were monitored, they found out that 1431 and 1541 pairs do not change much, while the icosahedral 1551 and 2331 pairs increased uniformly as the system being supercooled until a local maxima at 700 K, indicating the final state came to be stable amorphous state. Therefore, as the MG system is cooled from its liquid state, the icosahedral symmetry keeps increasing and this SRO structure has been proved a correlation with stability and generation of a MG system.

2.3. Voronoi tessellation

H-A analysis method can reveal the topology SRO structure effectively, but fail to obtain the specific geometry features of SRO structure. Voronoi tessellation is a polyhedral analysis method developed by introducing the concept of Voronoi polyhedral, which is defined as a closed convex polyhedral enclosed by the vertical bisectors of the nearest-neighbor atoms and center atom [10]. Usually, i_k is used to represent the number of polygon with k edges in a Voronoi polyhedral, and a four-number vector $< i_3, i_4, i_5, i_6 >$ is chosen as the Voronoi index, to describe the arrangement and symmetry of the nearest-neighbor atoms around the center atom. For example, an icosahedral with Voronoi index < 0,0,12,0 > has 12 pentagons enclosed, and a polyhedral with index < 0,3,6,0 > has 3 quadrilaterals and 6 pentagons enclosed. The polyhedral with same Voronoi index can be concluded as one type cluster. After analyzing all the local clusters compositions in MG, the motifs are summarized as a series of typical Voronoi polyhedral types and can be regard as mainly contributions to SRO structure.

Among these mentioned analysis methods, the Voronoi tessellation method is the most accurate and effective tool for typical structure identification in MGs, and also be used by many researchers [10–13]. Cheng et al. used this method to describe the structure evolution of Cu-Zr MG during quenching process [11]. Five most popular Voronoi polyhedral types were elected, which accounting for over 75% of all Cu-centered polyhedral. These clusters had common characteristics of high symmetry and a CN of 12, while the other fragmented clusters have low symmetry and usually irregular polyhedral with unfavorable CNs or highly distorted shapes. The polyhedral with Voronoi index < 0,0,12,0 > have a symmetrical fivefold geometry and icosahedral structure, and defined as "full icosahedra" (FI). FI clusters were found increase sharply during the quenching process, especially during the supercooled liquid regime. While the cluster motifs of MG with lower symmetry had a gradually change with the sample cooling. But the fragmental ones, which might the motifs of equilibrium liquid at melting temperature, decreased sharply accompanying with formation of glass state. These observations suggested that FI cluster mostly contributed to SRO and dominated the solid-like nature of MGs, and with lower cooling rate, the fraction of FI increased and made the generated MG a more stable one, which was consistent with glass formation cooling rate dependence. We will have a more detailed discuss on the cooling rate effect in Section 3.

2.4. MRO structures in MG

By combining experimental characterization tools such as XRD, EXAFS, and RMC together with *ab initio* simulation method, Sheng et al. resolved the MRO structure of various MGs [6]. With application of Voronoi tessellation, the formation of local solute-centered coordination polyhedral with strong chemical favoring unlike bonds was found and defined with "quasi-equivalent cluster". On the basis of the quasi-equivalent clusters, the MRO was further proposed to be dense packing of these clusters by sharing shell atoms, and regard as general feature of MG. Three basic icosahedra linkages were concluded as face-sharing (FS), edge-sharing (ES) and vertex-sharing (VS). **Figure 2** shows the typical connections of SRO and MRO structure in three MGs. Liu analyzed various MGs structure by PDF data and MD simulation. They indicated that the MRO structure can be interpreted as spherical-periodic

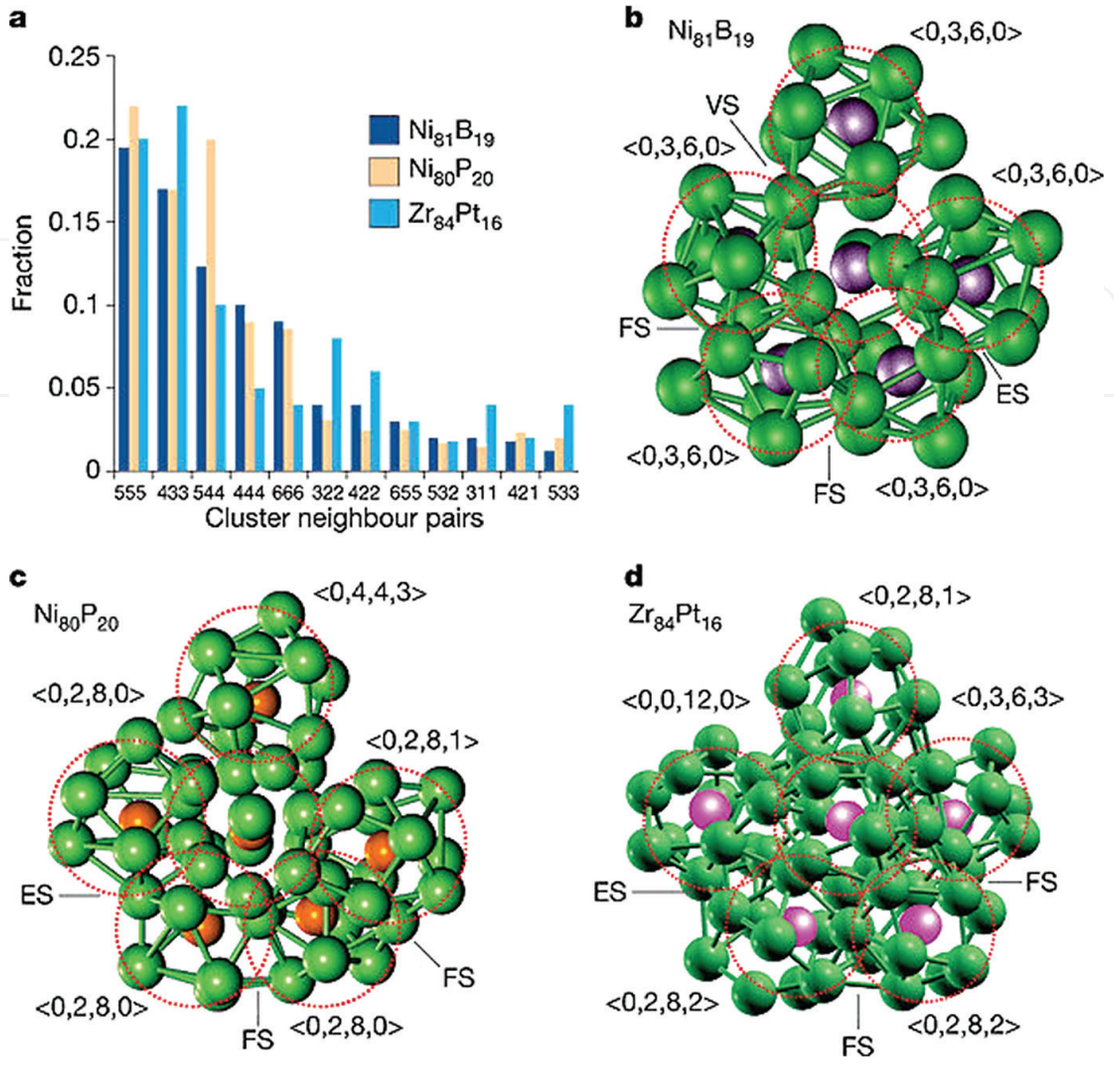

Figure 2. Typical connections of SRO clusters and MRO structures in MGs [6].

order and local translational symmetry, and the increasing of MRO structures proceeded throughout the glass transition process [14].

The combining of PDF and topological analysis method can also reveal the formation of MRO. Liang identified icosahedral clusters from an Mg-Zn MG using H-A analysis method, and found some neighbor clusters have linkage with structure packed and atoms shared [15]. The icosahedra linkages of intercross-sharing (IS), FS, ES, and VS were also detected. By evaluating the average distances between center atoms in each linking cluster, Liang found the distribution of the distances had a coincidence with the second peak splitting of PDF curve. With more clusters interacted into a network, MRO came to formation in the glass.

With the increase in simulation dimension, it was also found that the clusters tend to form large and interconnecting networks. Ward further extended the range of correlated packing of the icosahedral clusters, and found the diversities of the network diffusivity in compositions about the binary Cu-Zr MGs [12]. With 30% fraction of Zr atoms, the MG had higher fraction of Cu-centered FI clusters, which tended to form a single large network. With the promotion of

Zr atoms, the fraction of Cu-centered FI decreased severely, and the formed networks tended to be diffusive with decrease in size and increase in number. At 50% fraction for Zr atoms, the number of networks reached the maximum and had a downward tendency with the further increase of Zr atoms fraction. It was noted that the compositions of $Cu_{70}Zr_{30}$ and $Cu_{50}Zr_{50}$ both had high glass-forming ability, differences in network forming proved that the presence of networks is neither a sufficient nor necessary condition for the formation of glass phase, but networks formation does have dependence on the preparing procedures, and a strong effect on mechanical behavior of MG as well. The detailed explanation will be given in Section 3.

Another found by Cheng is that an addition of a small percentage of Al in the original Cu-Zr binary MG can lead to dramatically increased population of FI clusters and their spatial connectivity (shown in **Figure 3**) [12]. It has been known that the ideal icosahedral dense packing requires several factors: an atomic size ratio of 0.902 for a hard-packing model [16], and negative mixing heat of atoms. For binary Cu-Zr MG, the atomic size ratio is 0.804, Al atom has

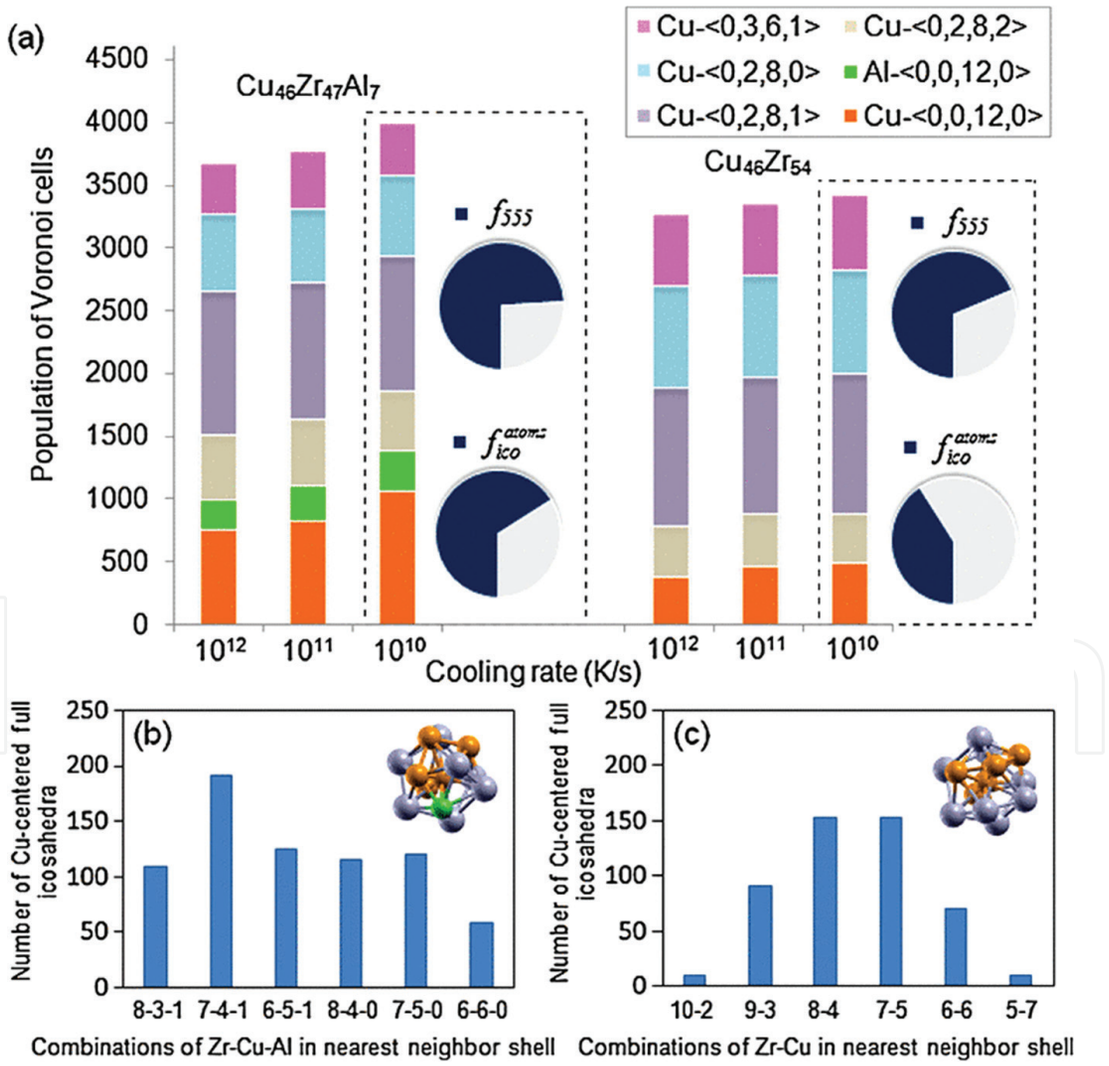

Figure 3. (a) Histogram showing differences in SRO components and fractions in Cu-Zr-Al ternary MG and Cu-Zr binary MG; (b) combinations of Cu-Zr-Al atoms in Cu-centered FI SRO in Cu-Zr-Al ternary MG and (c) Cu-Zr binary MG [13].

a radius in between of Zr and Cu atoms, the three atomic sizes can adjust the coordination polyhedron around the Cu atom, and increases the possibility of comfortable arrangements to reach FI. Furthermore, the negative mixing heat of Al with Zr and Cu drives Al to scatter in the Cu-Zr matrix. A more ideal ratio of 0.905 of Zr-Al atoms make Al surrounded by Zr become the topologically optimal way for FI packing. Similar with the binary Cu-Zr MG mentioned above, the FIs in this ternary MG overlapped and connected with the bonding forms of tetrahedral sharing (TS, same as IS), FS, ES, and VS, and then interconnected with each other resulting in the formation of networks (shown in **Figure 4**). The degree of connectivity of FI might serve as the backbone of the MG structures, and induced the more stable structure and improvement of mechanical properties in ternary glass compared with the binary glass. A further study taken by Tang suggested that those SRO clusters with low degree five-fold symmetry structure could also tend to form interconnected networks [17]. But different with the solid-like networks formed by FI clusters, the low five-fold symmetry clusters built up liquid-like networks. Compared with the solid-like networks, the liquid-like ones were less resistant to shear events and usually fertile sites for plastic deformation.

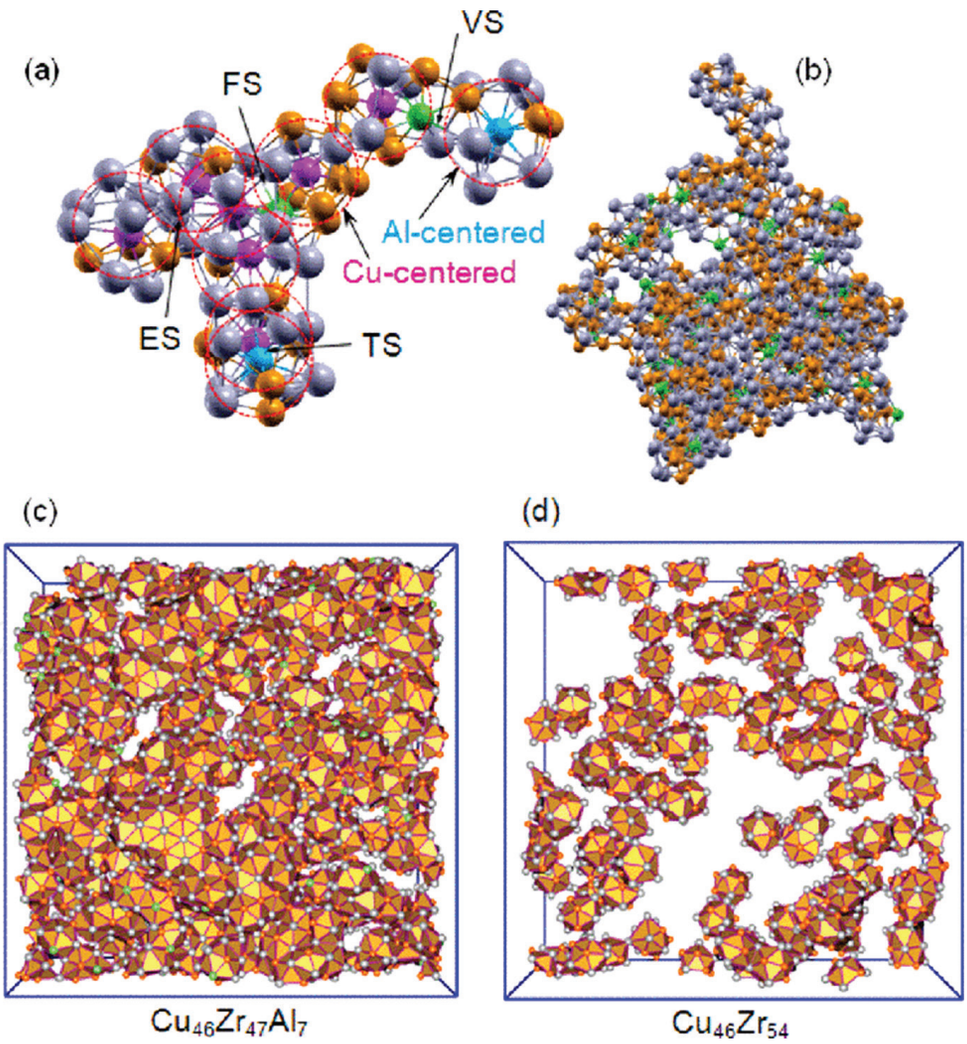

Figure 4. (a) A supercluster consisting four types of connections VS, ES, FS and TS; (b) a large supercluster consisting of over 700 atoms; (c) higher degree of connectivity of FI shown in Cu-Zr-Al MG compared with (d) Cu-Zr MG [13].

http://dx.doi.org/10.5772/intechopen.76830

3. Correlation of structure and mechanical properties

The correlation of structure and mechanical properties is a central theme of materials research, no matter crystalline materials or amorphous ones. The properties of MGs change pronouncedly with the internal structures change. Several works have been done for the influence of changes in composition proportions and variation in the processing conditions for MGs of a fixed composition, but what really governs the properties of MG from the sight of atomic-level structures has to be concerned for its quantitative and predictive theory establishment. The icosahedral cluster structures usually have a more dense packing efficiency, and the distributions are not even in space with connection of icosahedral existing. Thus, the MG structure has intrinsic fluctuations, and the local atomic-level area has heterogeneity in structure and dynamics, and the nanoscale mechanical heterogeneity had been proved with the using of dynamics force microscopy [18]. The mechanical response of MG sample can be significantly influenced by various local structure motifs, relative fractions, and their distributions in space. In other words, the structural heterogeneity necessarily leads to mechanical heterogeneity and decide the mechanical behavior of the MG [10, 19].

According to Wakeda's investigations on the shear deformation of Cu_xZr_{1-x} (x = 0.30–0.85) MGs, the local geometrical structures had large variation with the change of proportions, and affected the yield and fracture behavior of the MGs [20]. With application of Voronoi polyhedral analysis method, the local structures were characterized by pentagons and free volume, and these two factors were found related to each other. The pentagonal regions corresponded to the densely packed structure and nonpentagonal regions corresponded to the free volume structure. With shear simulation taken on the various MGs, it was found the pentagon-rich region tends to undergo elastic deformation, while the pentagon-poor was easily deformed plastically. Pentagon-rich local area had more formation of fivefold symmetry structure, and more relevant to the FI cluster, thus the aggregation of pentagons could be regard as formation of SRO. The results indicated the pentagonal SRO contributed the structural stability as well as elastic strength, while the opposite ones closely related to yield and fracture behavior in MGs.

The preparation processing of MG also has a significant influence on the formation of SRO cluster types and contents, and induces local SRO structure heterogeneity in MG. Cheng found that the mechanical behavior and dynamics responses varied with different cooling rates of MG [11]. When applied the same tensile loading procedure to the MG samples prepared under different cooling rates, the sample with lower cooling rate showed a strong tendency to form a single and highly localized SB, while the one with higher cooling rate had a more homogeneous deformation. To obtain a quantitative evaluation of strain localization, the degree of strain localization parameter was defined as:

$$\psi = \sqrt{\frac{1}{N}\sum_{i=1}^{N}\left(\eta_i^{Mises} - \eta_{ave}^{Mises}\right)^2}, \tag{2}$$

where, a larger ψ means larger fluctuations in the atomic strain and a more localized deformation mode. The strain localization degree ψ was found negatively correlated with cooling rates and positively correlated with the fraction of Cu-centered FI clusters. A shear deformation

simulation also showed the MG with lower cooling rate had higher shear stress compared with higher cooling rates. And the analysis on shear modulus showed a consistent tendency with strain localization phenomenon. These results showed the dynamics heterogeneity have a significant dependence on cooling rate, and revealed that the MG structure and mechanical behavior can be regulated by controlling the quenching process and cooling rates.

Since SBs formation is a significant signal for catastrophic failure of MG, the structure evolution analysis of SBs is necessary for the dynamics investigation during a deformation. Cao et al. studied the correlation of cluster evolution with the shear localization initiation in a Cu-Zr MG in the SB regime [21]. Fractions of several dominant cluster types in the SB forming region were analyzed during deformation, as shown in **Figure 5**. The breakdown of FI clusters was identified as a structural signature of the initiation of shear localization. With distorting of the FI backbone into less-shear-resistant, uncomfortable clusters, the shear localization propagating to a major SB with a velocity close to speed of voice. Feng et al. took quantitative treatment on the atomic structure of SBs in Cu-Zr MG and found the "liquid-like" features of SB [22]. With the method of H-A analysis, bonded pair types and distributions in SB are more similar to supercooled liquid compared with the MG matrix (shown in **Figure 6**). The SRO analysis results showed heterogeneous structure distribution in clusters. Zr-centered <0,2,8,5 > clusters exhibited strong spatial correlations and tendency to connect with each other in the SB, and formed interpenetrating solid-like backbone in SB (shown in **Figure 7**). Ju et al. took another view on the correlation of the mechanical properties and the local structural rearrangement of Mg-Zn-Ca MG by using H-A analysis method [23]. From the H-A index analysis on the system, the numbers of 1551 and 1431 local structures decreased with the increasing strain until 0.05, and the H-A indices of different types remained almost constant when the strain became larger than 0.05. The distributions of atomic local shear strain during the tension process showed the stages of the initialization of STZs, the extension of STZs, and the formation of shear bands along a direction 45° from the tensile direction.

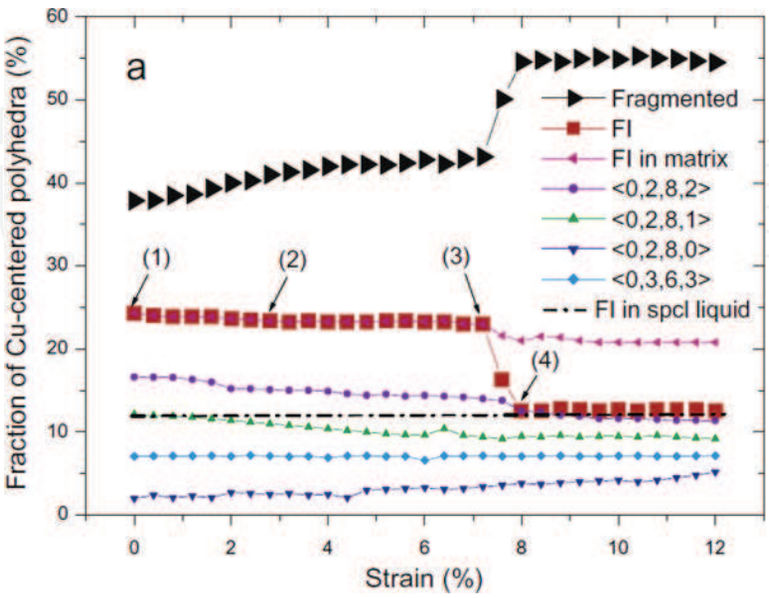

Figure 5. Variations of five dominant SRO clusters with the sample strain increasing in the SB region [21].

http://dx.doi.org/10.5772/intechopen.76830

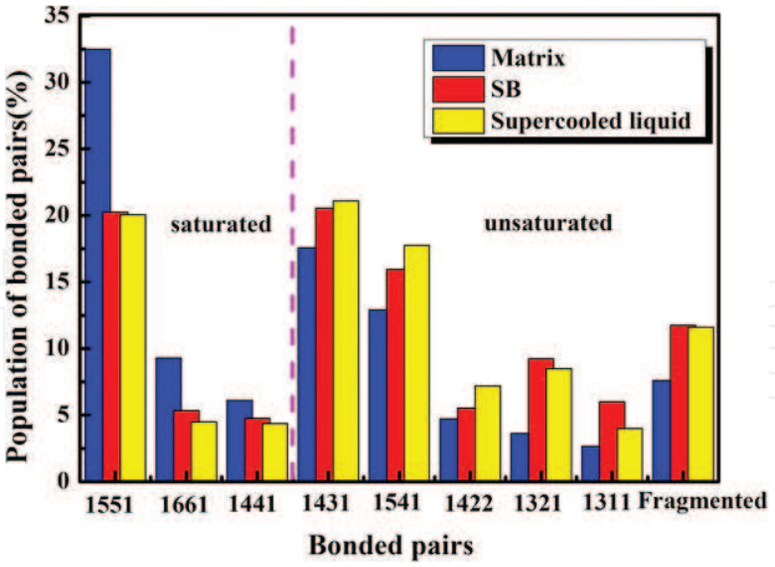

Figure 6. Comparison of several bonded pair types in the matrix, the SB, and supercooled liquid [22].

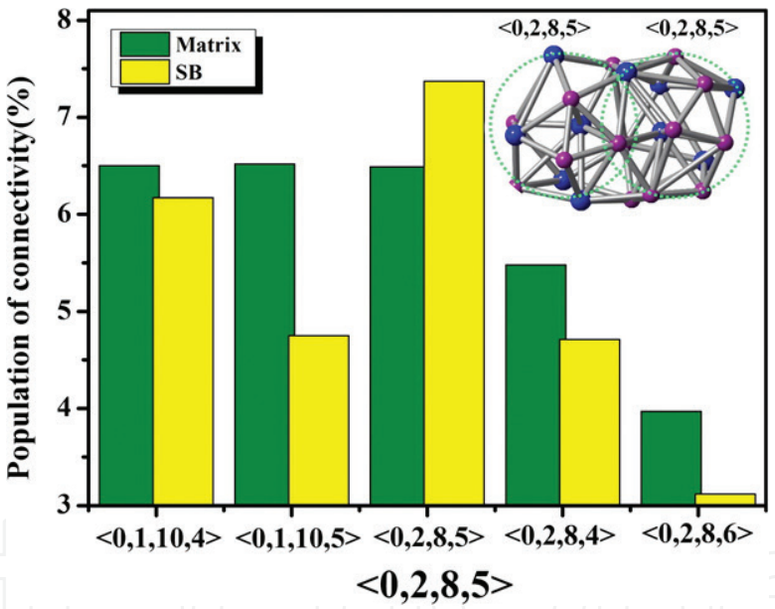

Figure 7. Connectivity of the network formed by the central atoms of the <0,2,8,5 > clusters [22].

The researching work about MG structure revealed the interconnection of icosahedra clusters was the intrinsic nature of MGs. The networks forming by neighboring icosahedra to medium range is negligible for the correlation of structure and mechanical properties in MGs. Lee et al. extended the structural hierarchy to a longer range by connecting MRO structures to large networks [24]. As we mentioned above, the MRO structures are constructed by connecting the neighboring SROs with each other. In Lee's works, interpenetrating connection of icosahedra (ICOI) structure was constructed by icosahedra, and it was illustrated as a typical MRO structure to explore correlation of structure and mechanical properties. To find out which pattern motif mostly contributed to structure stability, the potential energy of the center atom of the individual

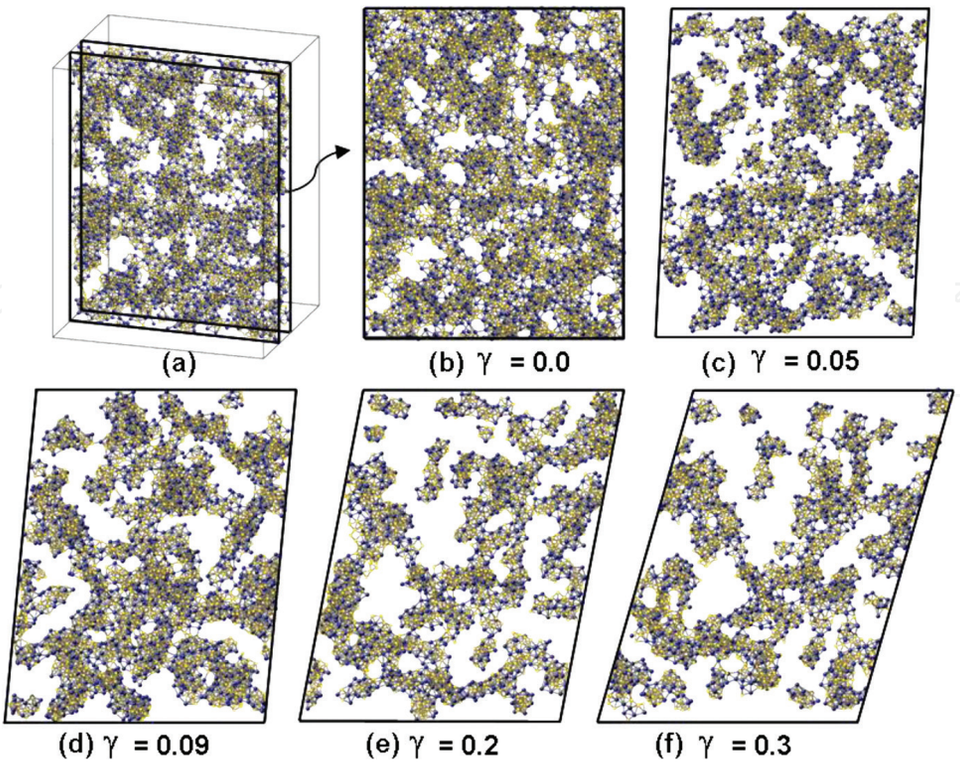

Figure 8. The breaking of ICOI networks in the during shear deformation [24].

icosahedra participating in the connection scheme of each patterns were calculated. It was found the icosahedra with volume shared type had a lower potential energy and stable structure, $Cu_{65}Zr_{35}$ had larger fractions of ICOIs with close connection of ICOIs compared to $Cu_{50}Zr_{50}$, and together with more dense atomic packing. With addition of shear simulations, $Cu_{65}Zr_{35}$ was found more resistant to applied load and showed higher elastic modulus and yield stress. The highly connected MROs constituted a compact icosahedral network over an extended range, which was resistant to stress-induced shear transformations under applied load. The breaking of ICOI networks during shear deformation are shown in **Figure 8**. This work presented the connectivity of MROs and showed its significant influence on the mechanical properties of MG.

4. Shear bands in MGs

This part moves on to a view of larger scale on the shear bands and their connection with the deformation of MGs, which is believed as a breakthrough of atom scale deformation in simulations with experimental phenomenon in macro scale. MGs have a similar performance in experiments with other amorphous materials such as silica glasses and polymers [25, 26], with blunt tip applied on the surface, typical slip line patterns will be shown in the cross surface, and the slip lines are regard caused by shear stress, thus called shear bands.

The formation and spreading of highly localized SBs is widely believed responsible for the failure of brittle MGs. But the ductile MGs could show homogeneous deformation without

http://dx.doi.org/10.5772/intechopen.76830

localization of SBs under the same mechanical loading. To describe the plastic flow and reveal the deformation transition mechanism, the initiation of SBs from a shear transformation is a fundamental problem for the starting. One of the most popular explanations is STZ theory raised by Argon [27]. According to the theory, STZs are the clusters composed of tens to hundreds of atoms, and the basic elements undergoing the plastic flow in MG. When a shear stress is applied on the MG, the atoms in the cluster have relative movements, and deformation takes place inside the cluster. The distortion of STZ is an activation process, and needs a certain activation energy and volume, to transfer a STZ from a high energy state to a lower one.

The propagation of a SB from a collection of STZs is next problem to be concerned. Ogata et al. performed shear deformation on Cu-Zr bulk MG with MD simulations [28], and observed the nucleation and localization of SBs during shear deformation. The nucleation of SB was taken place from a local atomic rearrangement like STZ, and this local deformation induced releasing of elastic strain energy in the shear plane, and activated the generation of more STZs. Then, the STZs interacted with each other and formed a SB in the shear direction. Furthermore, the generation of SB enhanced the elastic strain energy of the surrounding materials in the in-plane directions, made the spreading of SB more localized.

Shimizu et al. described the propagating and developing of SB as a growth process of embryonic shear band (ESB) [29, 30]. An ESB appeared at the concentrator of a group of activated STZs. When the far-field shear stress exceeds the glue traction with temperature rising induced by frictional heating, and the length of the ESB increased to a critical length over 100 nm, the ESB would become maturing to a localized SB. An aged-rejuvenation-glue-liquid (ARGL) SB model was used for the description of the shear front, and four zones were defined as aged glass, rejuvenated glass, glue, and liquid (illustrated in **Figure 9**). The temperature distributes from room temperature at aged glass end to over the glass transition temperature at the liquid end. Their model was supported by the temperature rising phenomenon, which can reach a maximum over 1000 K, can also be verified from the research work by Lewandowski et al. [31]. They planted a fusible tin coating to observe the temperature rise during bend-test on MG, and observed melting in the SBs formation area, thus deduced that local temperature rise in the bands can reach a few thousand kelvin.

For a further understanding on SBs, the mechanical properties of SBs were investigated by Zhou et al. by testing samples with pre-existing SBs with tensile MD simulations [32]. It was demonstrated that pre-deformation lowered material strength and triggered enhanced strain fluctuation before sample yielding, leading to highly dispersed plastic shearing in the entire

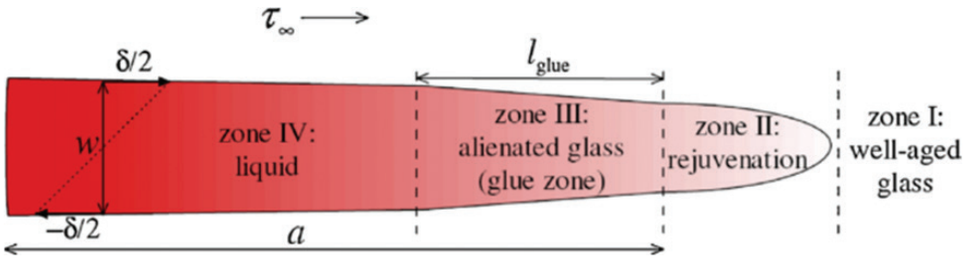

Figure 9. The aged-rejuvenation-glue-liquid (ARGL) shear band model [29].

sample. The transition in deformation mode from highly localized shear banding to nonlocalized plastic deformation was associated with the competition between the yield strength of the material and the critical stress required for the formation of mature SBs in the load-bearing materials. Zhong et al. extracted the SB part of a shear banding deformed MG, and applied tensile stress on the SB sample [33]. The SB tended to have softened tensile behavior and homogenous deformation, with lower tensile stress compared with MG matrix and no obvious localization of atomic strain.

Basing on the above investigation, the cavitation and propagation of SBs seems have a relation with various factors, such as size scale, cooling rate, temperature, composition, etc. Li et al. took MD simulations to investigate the tensile deformation behavior of MG samples with multimillion atoms [34]. They found small rob samples showed remarkable resistance to formation of SBs, and behaved unusual necking phenomenon. Three factors were concluded as contribution to the deformation mode size effects: surface effect, sample loading geometry, and finite sample size. With a further study on the shear banding behavior of double-notched sample, they indicated a critical dimension size about 10–20 nm was needed for the nucleation of SBs [35]. Gao et al. found the size effects in the deformation of Cu-Zr MG. With the model diameter gradually decreasing, the deformation mode of MG evolved from highly localized SB formation to homogenous deformation, but the stress increased significantly during the tensile process [36]. Zhong et al. also had an interest in the size effects, and they found with decreasing film thickness of MG, a transition from the localized deformation to the nonlocalized deformation indeed occurred [37]. Their further study revealed that the critical thickness for this transition was sensitive to the composition, and it was correlated with the average activation energy of the atomic level plastic deformation events [38].

Cheng et al. demonstrated the effects of cooling rate and composition on localization of deformation [11, 12]: with a lower cooling rate, the MG exhibited higher strength but easier trend to strain localization; the MG with composition of $Cu_{64}Zr_{36}$ with high proportion of FI clusters, was more resistant to the initiation of flows but increased propensity to strain localization, while $Cu_{40}Zr_{60}$ was on the opposite side. Zhong et al. utilized this property and created several composites by controlling the layers thickness and numbers of the two MGs, and investigated the deformation behavior of these composites [39]. They found out that MG samples with high layer numbers present obviously nonlocalized deformation behavior, the criterion for the deformation mode change for MGs was suggested as the competition between the elastic energy densities stored and the energy density needed for forming one mature SB in MGs. A further investigation on the annealing effects revealed that the localizing degree of SBs could also be regulated by annealing, with free volume deduction detected during the structural relaxation process [33]. Nanoindentation simulations on binary MG taken by Shi et al. also presented that the SB morphology under indenter had great dependence on indentation rate [40, 41]. At a lower loading rate, SBs showed wing-like morphology and easily propagated to the surface. In the opposite, wedge-like SBs came to formation and penetrated downward to MG matrix at higher loading rate. In our previous MD simulation work on Cu-Zr MG, we also observed more localized SBs under indentation at lower temperature, and more homogeneous deformation morphology at room temperature, which coincided with the brittleness characteristic of most MGs at low temperature [42].

The spreading of SBs can also be triggered or suppressed by cyclic loads, and it is relevant to soften or harden behaviors of MGs. Sha et al. performed MD simulations of tension-compression fatigue on $Cu_{50}Zr_{50}$ MG [43]. They observed the initiation and propagation of a major SB throughout the MG sample under cyclic loading. The cycling loads accelerated the accumulation of STZs, and triggered the spreading of SB once the aggregates of STZ reached the critical size for shear banding. Meanwhile, the fully formation of the SB was accompanied with stress drops, and this indicated the soften behavior of MG under uniform axial loads. While Deng et al. observed hardening behavior of Cu-Zr MG under cyclic indentation loads in MD simulations [44]. They indicated the post plastic deformation induced by the earlier indentations suppressed the SB formation by locally stiffening some portions of the original shear banding path, and then a higher load was needed for a secondary path of shear banding yield. Our works demonstrated this hardening behavior could be more severe under higher indentation loads or temperature [42]. In fact, these factors would induce higher plasticity in the deforming region, which formed more complex shear banding morphology and prevented localized SBs formation. These works performed that softening or hardening phenomenon could happen in MGs, due to SBs spreading or suppression under different types of cyclic loads.

5. Deformation behaviors of nanoglass

With highly inhomogeneous deformation dominated by localized SBs, MGs are easily encountered with catastrophically failure. Some pre-deformation process, like cold rolling, leads to a pseudocomposite structure consisting of a softer phase inside pre-induced SBs and a harder phase in the undeformed regions [45, 46]. These microstructural features improve the macroscopic plasticity by promoting the nucleation of secondary SBs and SB branching, as well as by limiting SB propagation due to the intersection of SBs. An alternative method to prevent a major SB development is regulating the volume-interface ratio and density by introducing particle interfaces into the matrix of MG [47]. Such a MG could be produced via cold compaction of glassy nanoparticles, and is therefore called a nanoglass (NG).

According to the definition of nanoglass, Sopu et al. constructed a 3D periodic Cu-Zr nanoglass with an idealized nanostructure consisting of columnar grains with a hexagonal cross section [48]. Applied with tensile stress during a mechanical test simulation, multiple embryonic SBs were formed along the interfaces and eventually started to propagate through the grain interiors in the NGs. Since the elastic energy was released homogeneously in the whole sample, the local energy release was not sufficient to accelerate any SBs; thus, NGs deformed homogeneously in contrast to the MGs, which exhibited localized deformation in one major SB, shown in **Figure 10**. Comparing the strain localization parameters of the NGs and MGs calculated according to Eq. (1), a more homogeneous deformation in the NGs was supported. Moreover, with an annealing treatment to the NGs, the glass particle interfaces seemed have a partial recovery of icosahedral SRO, led to the increase of strain localization.

Adibi et al. constructed a more random distributed NG by involving Poisson-Voronoi tessellation method, using the cast Cu-Zr MG structure as a source of material for the glassy grains

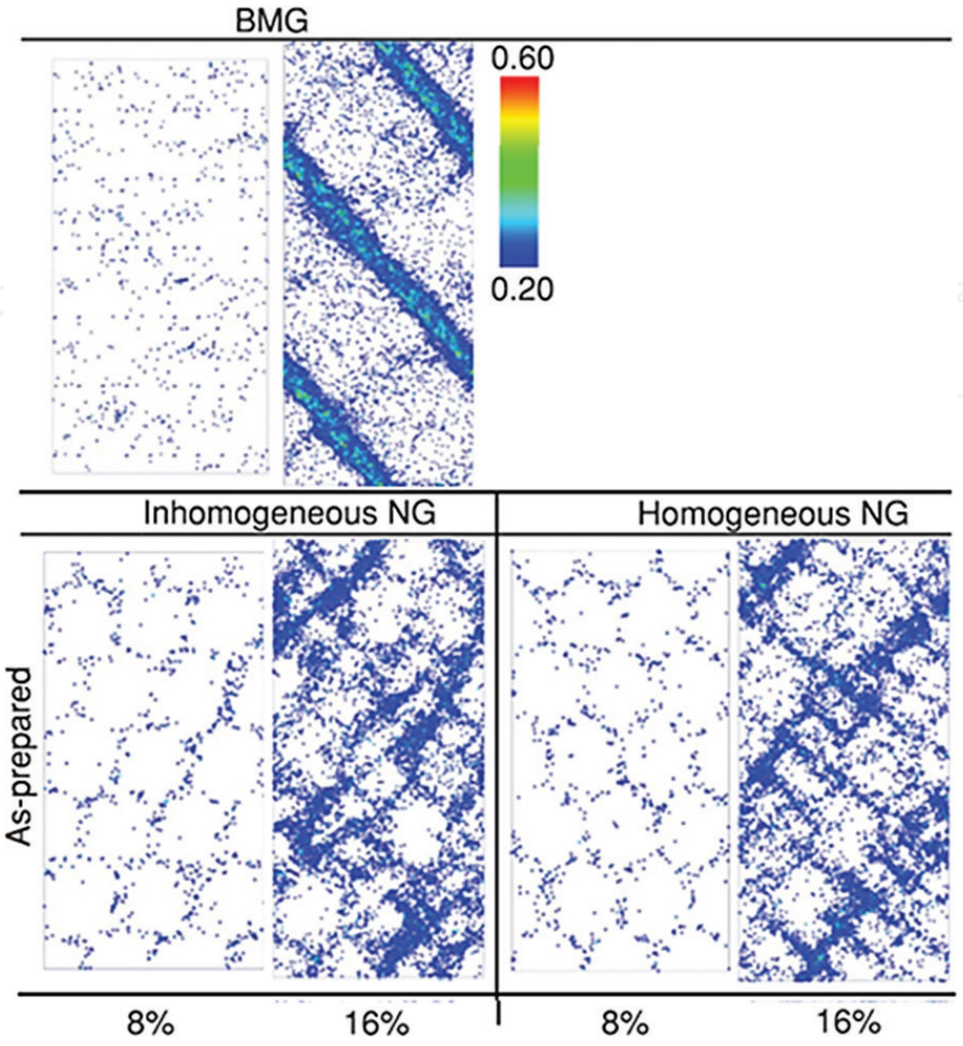

Figure 10. Local atomic shear strain distributions for MG, inhomogeneous NG and homogeneous NG at tensile of 8 and 16% [48].

(shown in **Figure 11**). Three specimens were selected with average glassy grain sizes from 5 to 15 nm to investigate deformation mode transition. The deformation modes of the NGs generally transferred from localized shear banding to homogeneous plastic flow with the grain sizes decreasing, and the fine-grained even became superplastically deformed during tensile testing [49]. The effects of composition and grain size were investigated more specifically by involving Voronoi polyhedral analysis method [50]. They found that the mechanical behavior of NGs was regulated by both the grain boundary thickness and the fraction of atoms at interfaces intrinsically. The mechanical behavior of NGs had a composition dependence similar to their parent MG, while the intrinsic deformation behavior only depended on the grain size, and not affected by the composition.

Sha et al. constructed a sandwich architecture composed of NG and MG [51]. The constructed composite had a higher strength than pure NG, and larger plasticity than MG. The improving of plasticity was contributed by the glass-glass interfaces in NG layers and a compressive residual stress in the MG layer. They indicated a strong ductile MG could be

http://dx.doi.org/10.5772/intechopen.76830

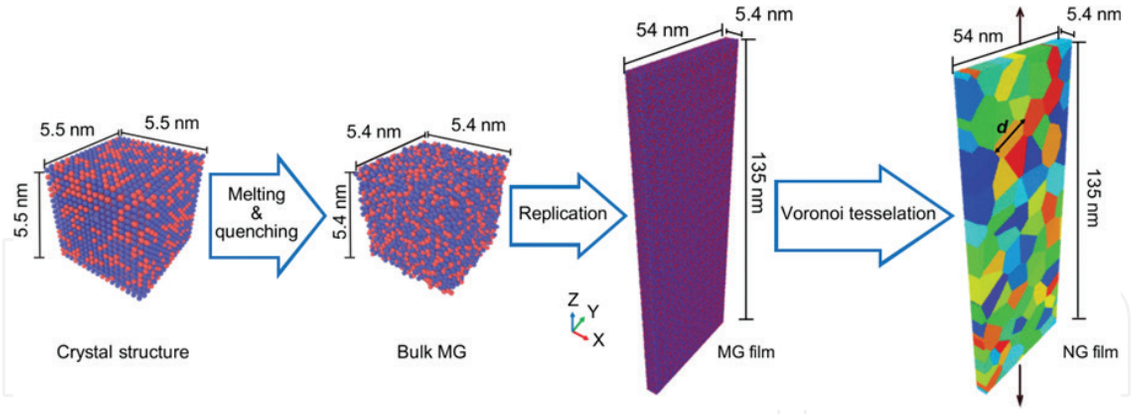

Figure 11. Schematic of the process to generate a NG film sample with Adibi's method [49].

constructed as sandwich architecture, and with a NG surface coated on the surface, MGs could be protected from localized SBs. They further conducted tensile load along the vertical direction to the laminates [52]. The change in the loading direction caused the differences not only in the location of SB initiation but also the critical distance between NG layers for failure mode transition. The MG-NG nanolaminate structure with NG layers closely packed and interfaces oriented parallel to the loading direction was identified as the most effective heterostructure. Adibi et al. constructed another NG-MG nanolaminates by combining layers of MG and NG [53], and further investigated mechanical properties of these nanopillar-shaped nanolaminates with tensile loading simulations. Compared with pure MG and NG, the MG-MG nanolaminate exhibited delayed SB formation and diffused shear banding failure, the NG-MG nanolaminate showed exceptional plasticity to a strain of 0.15 prior to a necking-type failure. These works suggest the MG composites constructed by NG and MG laminates can offer promise for creating structures that combine outstanding strength and ductility.

6. Conclusion and outlook

Throughout the review, we enumerated pronounced work on the structure analysis, the connection of structure with the mechanical properties, shear bands initiation and development. With the application of structural analysis methods, the existence of SRO and MRO in MGs is confirmed. The SRO types and proportions vary with MG compositions and preparation process. Several SRO motifs with high five-fold symmetry structure, as well as their interconnected networks, are found to be great contributing factors to the solid-like characteristics of MG, which means they are closely correlated with mechanical properties and deformation patterns of MGs. The intrinsic dynamics of shear banding events were investigated from the mechanics simulations, which provided convincingly supports for the shear banding theories. Furthermore, we also demonstrated recent MD simulations works on mechanical behaviors and deformation properties of several designed nanoglass. They behaved ductile deformation ability and might be a promising derived material from casted MGs.

These works proved the atomic-level computational simulation plays a significant role in researching work of MG. However, limited by accurate potential descriptions, computational capacity and simulation methods, computational simulations of MG are still unable to build a consistent theoretical frame with experimental research both in time and space. Thus, developing effective multi-scale simulation methods and advanced experimental characterization methods is the most urgent and challenging work for the research of metallic glasses.

Acknowledgements

This work was funded by the National Natural Science Funds for Excellent Young Scholar (51422503), Special Projects for Development of National Major Scientific Instruments and Equipment (2012YQ030075), Fund Guiding on Strategic Adjustment of Jilin Provincial Economic Structure Project (2014Z045), Major Project of Jilin Province Science and Technology development plan (20150203014GX), the special fund project of Jilin provincial industrial innovation (2016C030), Jilin Provincial Middle and Young Scientific and Technological Innovation Talent and Team Project (20170519001JH), Project (2017141) and Project (2017017) Supported by Graduate Innovation Fund of Jilin University.

Conflict of interest

The authors declared that they have no conflicts of interest to this work.

Author details

Hongwei Zhao*, Dan Zhao, Bo Zhu and Shunbo Wang

*Address all correspondence to: hwzhao@jlu.edu.cn

School of Mechanical Science and Engineering, Jilin University, Changchun, Jilin, China

References

[1] Gao YF. An implicit finite element method for simulating inhomogeneous deformation and shear bands of amorphous alloys based on the free-volume model. Modelling & Simulation in Materials Science & Engineering. 2006;**14**:1329-1345. DOI: 10.1088/0965-0393/14/8/004

[2] Yang Q, Mota A, Ortiz M. A finite-deformation constitutive model of bulk metallic glass plasticity. Computational Mechanics. 2006;**37**:194-204. DOI: 10.1007/s00466-005-0690-5

[3] Homer ER, Schuh CA. Mesoscale modeling of amorphous metals by shear transfo-rmation zone dynamics. Acta Materialia. 2009;**57**:2823-2833. DOI: 10.1016/j.actamat.2009.02.035

[4] Li L, Homer ER, Schuh CA. Shear transformation zone dynamics model for metallic glasses incorporating free volume as a state variable. Acta Materialia. 2013;**61**:3347-3359. DOI: 10.1016/j.actamat.2013.02.024

[5] Bernal JD. Geometry of the structure of monatomic liquids. Nature. 1960;**185**:68-70. DOI: 10.1038/185068a0

[6] Sheng HW, Luo WK, Alamgir FM, et al. Atomic packing and short-to-medium-range order in metallic glasses. Nature. 2006;**439**:419. DOI: 10.1038/nature04421

[7] Clarke AS, Jónsson H. Structural changes accompanying densification of random hard-sphere packings. Physical Review E Statistical Physics Plasmas Fluids & Related Interdisciplinary Topics. 1993;**47**:3975. DOI: 10.1103/PhysRevE.47.3975

[8] Honeycutt JD, Andersen HC. Molecular dynamics study of melting and freezing of small Lennard-Jones clusters. Journal of Physical Chemistry. 1987;**91**:4950-4963. DOI: 10.1021/j100303a014

[9] Duan G, Xu D, Zhang Q, et al. Molecular dynamics study of the binary $Cu_{46}Zr_{54}$ metallic glass motivated by experiments: Glass formation and atomic-level structure. Physical Review B. 2005;**71**:224208. DOI: 10.1103/PhysRevB.71.224208

[10] Cheng YQ, Sheng HW, Ma E. Relationship between structure, dynamics, and mechanical properties in metallic glass-forming alloys. Physical Review B. 2008;**78**:014207. DOI: 10.1103/PhysRevB.78.014207

[11] Cheng YQ, Cao AJ, Ma E. Correlation between the elastic modulus and the intrinsic plastic behavior of metallic glasses: The roles of atomic configuration and alloy composition. Acta Materialia. 2009;**57**:3253-3267. DOI: 10.1016/j.actamat.2009.03.027

[12] Ward L, Miracle D, Windl W, et al. Structural evolution and kinetics in Cu-Zr metallic liquids from molecular dynamics simulations. Physical Review B. 2013;**88**:134205. DOI: 10.1103/PhysRevB.88.134205

[13] Cheng YQ, Ma E, Sheng HW. Atomic level structure in multicomponent bulk metallic glass. Physical Review Letters. 2009;**102**:245501. DOI: 10.1103/PhysRevLett.102.245501

[14] Liu XJ, Xu Y, Hui X, et al. Metallic liquids and glasses: Atomic order and global packing. Physical Review Letters. 2010;**105**:155501. DOI: 10.1103/PhysRevLett.105.155501

[15] Liang YC, Liu RS, Mo YF, et al. Influence of icosahedral order on the second peak splitting of pair distribution function for $Mg_{70}Zn_{30}$ metallic glass. Journal of Alloys & Compounds. 2014;**597**:269-274. DOI: 10.1016/j.jallcom.2014.01.052

[16] Nelson DR, Spaepen F. Polytetrahedral order in condensed matter. Solid State Physics. 1989;**42**:1-90. DOI: 10.1016/S0081-1947(08)60079-X

[17] Tang C, Wong CH. A molecular dynamics simulation study of solid-like and liquid-like networks in $Zr_{46}Cu_{46}Al_8$ metallic glass. Journal of Non-Crystalline Solids. 2015;**422**:39-45. DOI: 10.1016/j.jnoncrysol.2015.05.003

[18] Liu YH, Wang D, Nakajima K, et al. Characterization of nanoscale mechanical heterogeneity in a metallic glass by dynamic force microscopy. Physical Review Letters. 2011; **106**:125504. DOI: 10.1103/PhysRevLett.106.125504

[19] Cheng YQ, Ma E. Atomic-level structure and structure–property relationship in metallic glasses. Progress in Materials Science. 2011;**56**:379-473. DOI: 10.1016/j.pmatsci.2010.12.002

[20] Wakeda M, Shibutani Y, Ogata S, et al. Relationship between local geometrical factors and mechanical properties for cu–Zr amorphous alloys. Intermetallics. 2007;**15**:139-144. DOI: 10.1016/j.intermet.2006.04.002

[21] Cao AJ, Cheng YQ, Ma E. Structural processes that initiate shear localization in metallic glass. Acta Materialia. 2009;**57**:5146-5155. DOI: 10.1016/j.actamat.2009.07.016

[22] Feng S, Qi L, Wang L, et al. Atomic structure of shear bands in $Cu_{64}Zr_{36}$ metallic glasses studied by molecular dynamics simulations. Acta Materialia. 2015;**95**:236-243. DOI: 10.1016/j.actamat.2015.05.047

[23] Ju SP, Huang HH, Wu TY. Investigation of the local structural rearrangement of $Mg_{67}Zn_{28}Ca_5$ bulk metallic glasses during tensile deformation: A molecular dynamics study. Computational Materials Science. 2015;**96**:56-62. DOI: 10.1016/j.commatsci.2014.09.005

[24] Lee M, Lee CM, Lee KR, et al. Networked interpenetrating connections of icosahedra: Effects on shear transformations in metallic glass. Acta Materialia. 2011;**59**:159-170. DOI: 10.1016/j.actamat.2010.09.020

[25] Jeong HY, Li XW, Yee AF, et al. Slip lines in front of a round notch tip in a pressure-sensitive material. Mechanics of Materials. 1994;**19**:29-38. DOI: 10.1016/0167-6636(94)90035-3

[26] Su C, Anand L. Plane strain indentation of a Zr-based metallic glass: Experiments and numerical simulation. Acta Materialia. 2006;**54**:179-189. DOI: 10.1016/j.actamat.2005.08.040

[27] Argon AS. Plastic deformation in metallic glasses. Acta Metallurgica. 1979;**27**:47-58. DOI: 10.1016/0001-6160(79)90055-5

[28] Ogata S, Shimizu F, Li J, et al. Atomistic simulation of shear localization in Cu–Zr bulk metallic glass. Intermetallics. 2006;**14**:1033-1037. DOI: 10.1016/j.intermet.2006.01.022

[29] Shimizu F, Ogata S, Li J. Yield point of metallic glass. Acta Materialia. 2006;**54**:4293-4298. DOI: 10.1016/j.actamat.2006.05.024

[30] Shimizu F, Ogata S, Li J. Theory of shear banding in metallic glasses and molecular dynamics calculations. Materials Transactions. 2007;**48**:2923-2927. DOI: 10.2320/matertrans. MJ200769

[31] Lewandowski JJ, Greer AL. Temperature rise at shear bands in metallic glasses. Nature Materials. 2006;**5**:15-18. DOI: 10.1038/nmat1536

[32] Zhou HF, Zhong C, Cao QP, et al. Non-localized deformation in metallic alloys with amorphous structure. Acta Materialia. 2014;**68**:32-41. DOI: 10.1016/j.actamat.2014.01.003

[33] Zhong C, Zhang H, Cao QP, et al. Deformation behavior of metallic glasses with shear band like atomic structure: A molecular dynamics study. Scientific Reports. 2016;**6**:30935. DOI: 10.1038/srep30935

[34] Li QK, Li M. Free volume evolution in metallic glasses subjected to mechanical deformation. Materials Transactions. 2007;**48**:1816-1821. DOI: 10.2320/matertrans.MJ200785

[35] Li QK, Li M. Assessing the critical sizes for shear band formation in metallic glasses from molecular dynamics simulation. Applied Physics Letters. 2007;**91**:231905. DOI: 10.1063/1.2821832

[36] Gao LK, Zhao FL, Xu N, et al. Size effects: The relation to the percentage of atoms that participate in the deformation of ZrCu metallic glass. Journal of Spectroscopy. 2014;**2014**:1-5. DOI: 10.1155/2014/627679

[37] Zhong C, Zhang H, Cao QP, et al. The size-dependent non-localized deformation in a metallic alloy. Scripta Materialia. 2015;**101**:48-51. DOI: 10.1016/j.scriptamat.2015.01.015

[38] Zhong C, Zhang H, Cao QP, et al. On the critical thickness for non-localized to localized plastic flow transition in metallic glasses: A molecular dynamics study. Scripta Materialia. 2016;**114**:93-97. DOI: 10.1016/j.scriptamat.2015.12.012

[39] Zhong C, Zhang H, Cao QP, et al. Non-localized deformation in Cu-Zr multi-layer amorphous films under tension. Journal of Alloys & Compounds. 2016;**678**:410-420. DOI: 10.1016/j.jallcom.2016.03.305

[40] Shi Y, Falk ML. Simulations of nanoindentation in a thin amorphous metal film. Thin Solid Films. 2007;**515**:3179-3182. DOI: 10.1016/j.tsf.2006.01.032

[41] Shi Y, Falk ML. Stress-induced structural transformation and shear banding during simulated nanoindentation of a metallic glass. Acta Materialia. 2007;**55**:4317-4324. DOI: 10.1016/j.actamat.2007.03.029

[42] Zhao D, Zhao HW, Zhu B, et al. Investigation on hardening behavior of metallic glass under cyclic indentation loading via molecular dynamics simulation. Applied Surface Science. 2017;**416**:14-23. DOI: 10.1016/j.apsusc.2017.04.125

[43] Sha ZD, Qu SX, Liu ZS, et al. Cyclic deformation in metallic glasses. Nano Letters. 2015;**15**:7010-7015. DOI: 10.1021/acs.nanolett.5b03045

[44] Deng C, Schuh CA. Atomistic mechanisms of cyclic hardening in metallic glass. Applied Physics Letters. 2012;**100**:4067. DOI: 10.1063/1.4729941

[45] Lee MH, Lee KS, Das J, et al. Improved plasticity of bulk metallic glasses upon cold rolling. Scripta Materialia. 2010;**62**:678-681. DOI: 10.1016/j.scriptamat.2010.01.024

[46] Cao QP, Liu JW, Yang KJ, et al. Effect of pre-existing shear bands on the tensile mechanical properties of a bulk metallic glass. Acta Materialia. 2010;**58**:1276-1292. DOI: 10.1016/j.actamat.2009.10.032

[47] Jing J, Krämer A, Birringer R, et al. Modified atomic structure in a Pd-Fe-Si nanoglass: A Mössbauer study. Journal of Non-Crystalline Solids. 1989;**113**:167-170. DOI: 10.1016/0022-3093(89)90007-0

[48] Şopu D, Ritter Y, Gleiter H, et al. Deformation behavior of bulk and nanostructured metallic glasses studied via molecular dynamics simulations. Physical Review B. 2011;**83**. DOI: 10.1103/PhysRevB.83.100202

[49] Adibi S, Sha ZD, Branicio PS, et al. A transition from localized shear banding to homogeneous superplastic flow in nanoglass. Applied Physics Letters. 2013;**103**:. 211905-211905-5. DOI: 10.1063/1.4833018

[50] Adibi S, Branicio PS, Zhang YW, et al. Composition and grain size effects on the structural and mechanical properties of CuZr nanoglasses. Journal of Applied Physics. 2014;**116**:2744. DOI: 10.1063/1.4891450

[51] Sha ZD, He LC, Pei QX, et al. The mechanical properties of a nanoglass/metallic glass/nanoglass sandwich structure. Scripta Materialia. 2014;**83**:37-40. DOI: 10.1016/j.scriptamat. 2014.04.009

[52] Sha ZD, Branicio PS, Lee HP, et al. Strong and ductile nanolaminate composites combining metallic glasses and nanoglasses. International Journal of Plasticity. 2017;**90**:231-241. DOI: 10.1016/j.ijplas.2017.01.010

[53] Adibi S, Branicio PS, Ballarini R. Compromising high strength and ductility in nanoglass–metallic glass nanolaminates. RSC Advances. 2016;**6**:13548-13553. DOI: 10.1039/C5RA24715B